



Open Access: ISSN 1847-9286

<https://pub.iapchem.org/ojs/index.php/JESE>

Original scientific paper

Simultaneous determination of trace levels of Cd(II) and Pb(II) in tap water samples by anodic stripping voltammetry with 2-mercaptobenzothiazole modified electrode

Sophy Phlay¹, Weena Aemaeg Tapachai², Supunee Duangthong¹, Puchong Worattananurak¹ and Pipat Chooto^{1,✉}

¹Analytical Chemistry Division, Department of Chemistry, Faculty of Science, Prince of Songkla University, Hatyai, Songkhla, 90112, Thailand

²Inorganic Chemistry Division, Department of Chemistry, Faculty of Science, Prince of Songkla University, Hatyai, Songkhla, 90112, Thailand

Corresponding author: ✉ pipat.c@psu.ac.th

Received: December 12, 2018; Revised: May 7, 2019; Accepted: May 9, 2019

Abstract

Glassy carbon electrode (GCE) modified by 2-mercaptobenzothiazole (MBT), mesoporous silica (Meso) and bismuth was developed to determine Cd(II) and Pb(II) simultaneously by square wave anodic stripping voltammetry (SWASV). In-situ preparation was found to work best in optimum conditions of acetate buffer pH 6, accumulation potential of -1.1 V, deposition time of 300 s and scan rate of 200 mV/s. SW peaks revealed the linear range of 5-50 µg/L Cd(II) and 5-50 µg/L Pb(II). LOD and LOQ for Cd(II) and Pb(II) were determined as 0.56, 0.80, 1.87 and 2.66 µg/L, respectively. The interaction of metals with bismuth and MBT, as well as higher surface area due to mesoporous silica, support beneficial performance of the modified electrode. Insignificant interferences from other regularly present metal ions were found. With SRM1640 standard, the SWASV results are found comparable to those obtained by inductive coupled plasma optical emission spectrometry (ICP-OES). The method was used to analyze the metals in tap water by standard addition method with the satisfactory recovery of 100.7 % for Cd(II) and 100.8 % for Pb(II).

Keywords

Modified electrodes; 2-mercaptobenzothiazole; Square wave anodic stripping voltammetry

Introduction

Among heavy metals with high potential in contamination of water for daily consumptions are Cd(II) and Pb(II). At present, the contamination problems from both metals are still found in a number of areas all over the world. The main source of Cd(II) is from discarded batteries, whereas

Pb(II) can contaminate water *via* dyes, paints, pipes and solders. It has been known that these metals can occur together and cause more damage especially to the brain [1,2]. The limits set by USEPA are 0.005 mg/L for Cd(II) and 0.015 mg/L for Pb(II) [3]. The techniques which are cost-effective, fast, simple and sensitive are therefore required in testing water samples. Even though there are a number of possibilities, a reference technique that can be applied for simultaneous determination of Pb(II) and Cd(II) in problematic areas around the world is still a matter of challenge. Traditional methods with high sensitivity have usually been used in laboratory conditions for the detection of Pb(II) and Cd(II), such as UV–vis spectrophotometry [4], fluorescence method [5], ion-selective electrode [6], graphite furnace atomic absorption spectrometry [7], atomic emission spectroscopy [8,9] and inductively coupled plasma mass spectrometry [10]. However, these techniques have the drawbacks of being time-consuming, complex, expensive and not suitable for onsite analysis.

With electrode modification by organic compounds, polymers and nanomaterials, electrochemical methods, especially anodic stripping voltammetry (ASV), can provide some advantages including speed, accuracy, sensitivity, selectivity, reproducibility and stability [11]. Boron doped diamond electrode (BDD) [12] was found to work well with Pb(II) and its modification with 4-aminomethyl benzoic acid provided figures of merits for Cd(II) analysis [13]. For simultaneous determination of Cd(II) and Pb(II), the most widely investigated is the use of bismuth which forms alloys with both metals [14,15]. Satisfactory LOD values were especially obtained when Bi was coupled with various materials such as carbon nanotubes in order to facilitate formation of larger surface areas. A variety of compounds such as graphene [16], Co₃O₄ [17], polymers [18,19] and crown ether [20,21] were also found to be successful in pre-concentrating both metal ions. Organic ligands with electron rich atoms including phytic acid oxygen [22,23], phenolic oxygen and nitrogen [24], cysteine sulfur [25,26] and lysine nitrogen [27] were found to implement better analytical performances for simultaneous determination of Cd(II) and Pb(II). MBT is an alternative ligand containing nitrogen and sulfur [28] which was used in the extraction of both metals before analysis by flame atomic absorption spectroscopy (FAAS) [29], as a biosensor for pesticides [30] and in forming polymeric structure to accommodate more complexing sites [31].

This paper reports an investigation of using MBT modified electrode for the first time to analyze Pb(II) and Cd(II) simultaneously by an ASV technique. The method is optimized, verified and then applied to the real samples.

EXPERIMENTAL

Reagents and samples

All reagents were used as received without any further treatment. Cd(II) and Pb(II) standards were prepared in-house from their nitrate salts as an atomic spectroscopy standard solution. Tetrabutylammonium hexafluorophosphate with the purity of $\geq 98.0\%$ and bismuth (III) nitrate pentahydrate were obtained from Fluka, whereas 2-mercaptobenzothiazole and mesoporous silica were from Sigma-Aldrich. Other reagents and metal salts for interference studies were of the highest purity commercially available. All subsequent solutions were prepared with deionized water (resistivity not less than 18 M Ω cm, ELGA water purification system, England) and purged by nitrogen gas (99.99%) for 2 min before use. Laboratory glassware was cleaned with 10% (v/v) nitric acid solution and then rinsed with deionized water. Cd(II) and Pb(II) standard solutions were prepared by diluting the respective stock solutions with the high purity deionized water and stored in polyethylene bottles before use.

NIST (National Institute of Standards and Technology) SRM 1640 composed of natural fresh water from Clear Creek, Colorado USA, was used as a reference with the certified value of $22.79 \pm 0.96 \mu\text{g/L}$ Cd(II) and $27.89 \pm 0.14 \mu\text{g/L}$ Pb(II).

Tap water samples were collected in different spots within the city of Hatyai, Songkhla, Thailand, digested by mixing the aliquot of 500 mL with 2 mL of concentrated HNO_3 and 2 mL of KNO_3 , put in cleaned polyethylene bottles and kept at 4°C before analysis.

Instrumentation

A PowerLab 2/20 with Potentiostat (ADInstrument, Australia) and EChem software was used for cyclic voltammetry (CV) and square wave anodic stripping voltammetry (SWASV), whereas Metrohm AUTOLAB PGSTAT 302N with NOVA software was used for EIS measurements. An Ag/AgCl, 3 M KCl reference electrode (Metrohm), a platinum counter electrode (Metrohm) and a modified glassy carbon electrode (Windsor Scientific Ltd., UK) with an inner diameter of 3 mm put in 50 mL cell were used for electrochemical measurements. All voltages were reported versus Ag/AgCl reference electrode. pH was measured by pH meter Model 510 (Eutech Instruments, USA) and inductively coupled plasma optical emission spectrometer (ICP-OES) Optima 4300 DV (Perkin-Elmer, USA) was used for the comparison of methods.

Preparation of modified electrode and starting procedure

The modified electrodes with different compositions and different orders of mixing were tested to select the one with the best sensitivity enhancement. Differential pulse (DP) and square wave (SW) results, as well as electrodes modified by in-situ and ex-situ Bi deposition were also compared. The following starting procedure was designed for further optimization:

Three electrodes were put in 50 mL cell containing 50 mL of 0.1 M acetate buffer pH 6. Then, $0.1 \mu\text{g/L}$ Cd(II) and Pb(II), $200 \mu\text{g/L}$ Bi(III), 1000 mg/L Meso and 1000 mg/L MBT were added into solution. The metals were then deposited under the initial conditions of -1.4 V for 300 s with stirring. After the equilibration time of 30 s, SWASV potential was scanned from -1.0 to -0.2 V with the scan rate of 250 mV/s , frequency of 50 Hz, amplitude of 75 mV and potential step of 160 mV to obtain the stripping current signals for analysis. Optimization was conducted by varying a number of parameters (*vide infra*) for the best analytical performance to be used in real sample analysis.

Results and discussion

Electrode modification and voltammograms of Cd(II) and Pb(II)

A number of modification experiments has been conducted to figure out the most suitable materials and methods. Ex-situ Bi deposition was found to result in a lower current value and unsymmetrical peak shape. As shown in Figure 1, the best sensitivity was obtained for in-situ modified GCE in the order of Bi + Meso + MBT. The results reflect the role of Meso in increasing surface areas and sites, and role of Bi and MBT in alloy forming and complexation, respectively. Within the potential range of -1.0 to -0.2 V applied after the starting procedure, two well defined stripping peaks at Bi + Meso + MBT modified electrode were observed at -0.72 V for Cd(II) and -0.58 V for Pb(II), and the enhancement of stripping currents can be clearly seen for both metal ions. This kind of electrode modification was therefore used for further optimization, verification and analysis.

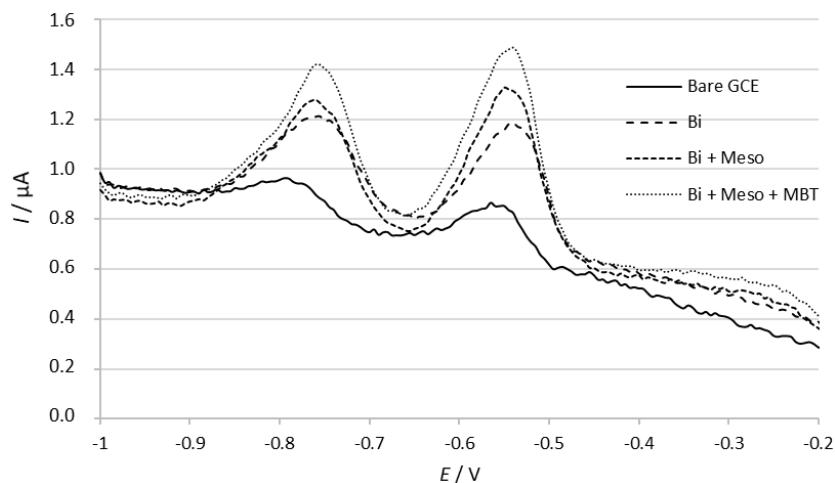


Figure 1. Comparison of stripping currents of 0.1 mg/L Cd(II) and Pb(II) at differently modified electrodes in conditions of 0.1 M acetate buffer pH 6, deposition potential -1.4 V, deposition time 300 s, equilibration time 30 s and concentrations of Meso 1000 mg/L, MBT 1000 mg/L and Bi 0.2 mg/L.

CV and EIS for electrode characterizations

Figure 2 shows the cyclic voltammetry (CV) results of differently modified GCEs in acetate buffer solution containing Ru(NH₃)₆³⁺ (a) and Fe(CN)₆⁴⁻ (b). It is clear that each modification step of GCE supports the electron transfer well for both inner and outer spheres by maintaining reversibility and increasing the current.

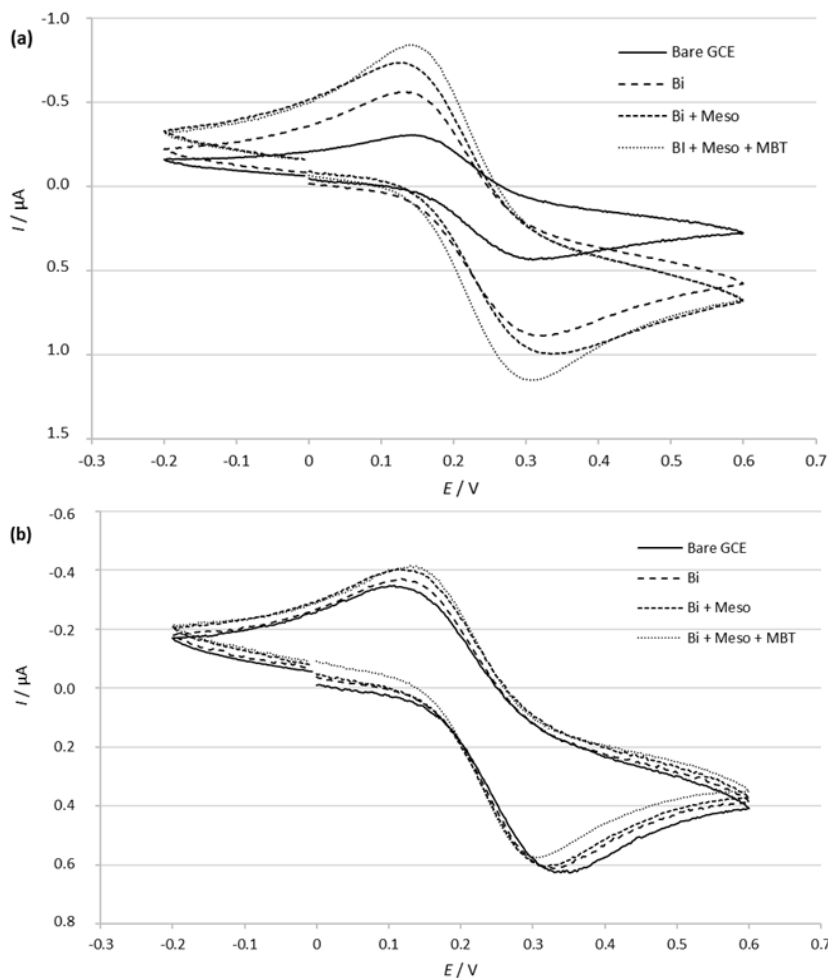


Figure 2. Cyclic voltammetry for bare GCE, Bi/GCE, Meso-Bi/GCE and Bi-Meso-MBT/GCE, with scan rate 100 mV/s in 0.1 M acetate buffer containing 2.5 mM Ru(NH₃)₆³⁺ (a) and Fe(CN)₆⁴⁻ (b).

The electron transfer capacities of modified electrodes were characterized by electrochemical impedance spectroscopy (EIS). Less curvature in an impedance spectrum is well known to represent less resistance to electron transfer. Therefore, Figure 3 reveals that addition of each modifying agent facilitates the electron transfer exhibiting less resistance, and the effect is highest after addition of MBT.

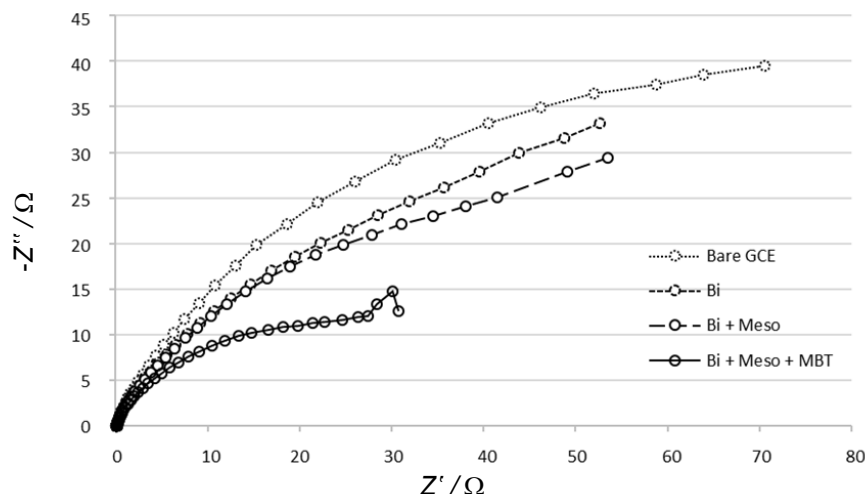


Figure 3. Impedance spectra of the bare GCE, Bi/GCE, Bi-Meso/GCE, Bi-Meso-MBT/GCE.

Optimization

Comparison of SWASV and DPASV

SWASV and DPASV parameters are summarized in Table 1. Comparison of corresponding stripping currents is presented in Figure 4, showing higher current enhancement in the case of SWASV. Hence, SWASV technique is selected for the following experiments.

Table 1. SWASV and DPASV parameters

Parameter	SWASV	DPASV
Accumulation step		
Deposition potential	-1000 mV	-1000 mV
Deposition time	400 s	800 s
Equilibration time	30 s	30 s
Measuring Step		
Frequency	50 Hz	-
Step potential	160 mV	100 mV
Amplitude	75 mV	75 mV

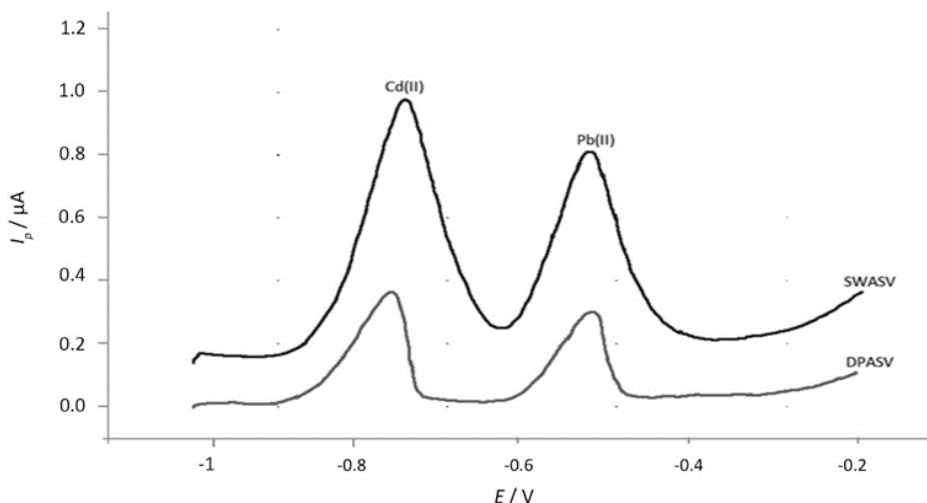


Figure 4. Comparison of stripping currents of 0.1 mg/L Cd(II) and Pb(II) from SWASV and DPASV.

Effect of pH

Within the experimental pH range of 1 to 7, the maximum peak current for both metals was obtained at pH 6 as shown in Figure 5(a) and this value was used for the next investigations. pH 6 is suitable for the formation of sulfide anions of MBT to form complexes with metal ions corresponding with pKa of 6.93 [32]. If pH is lower than 6, protonation causes the formation of sulfhydryl groups which make complex formation more difficult. At pH higher than 6, the metals are probably susceptible to form hydroxides.

Deposition potential

The influence of deposition potentials was investigated over the potential range of -0.1 to -1.5 V. As shown in Figure 5(b), the current firstly increased steeply up to -1.1 V and then became almost constant. This is due to the greater extent of metal accumulation until the potential was high enough for deposition of both metals. Beyond -1.4 V, the current started to drop, possibly because greater thickness slows down the mass transfer and higher negative potential is susceptible to side reactions. The highest current for both metals is found at -1.1 V which was fixed for metal electrodeposition for the following study.

Deposition time

The deposition time was varied from 100 to 500 s. As shown in Figure 5(c), the current values gradually increased with time up to 300 s because greater accumulation of bismuth facilitated formation of alloys until surface saturation was reached. However, the current dropped before it went up again, reflecting that certain time is needed for alloy rearrangement. The highest peak current was found at 300 s and this was used for further optimizations and applications.

Effect of Bi concentration

The concentration of Bi was varied from 100 to 500 $\mu\text{g/L}$. Figure 5(d) reveals firstly a normal trend of increasing current which is due to the increase of film thickness and then the current decreased because greater thickness can inhibit the mass transfer during the stripping step [33]. The concentration of 200 $\mu\text{g/L}$ provided the greatest peak current for both metals and was therefore selected for the following experiments.

Effect of Meso concentration

As shown in Figure 5(e), similar trend is obtained when Meso concentrations were changed from 100 to 600 $\mu\text{g/L}$. Similar to previous explanation of the effect of Bi concentration, the excess of Meso can result in less current due to the obstruction of mass transfer. The concentration of 300 $\mu\text{g/L}$ showing the greatest current was chosen for further investigations.

Effect of MBT concentration

As shown in Figure 5(f), within the studied range of 100 to 600 $\mu\text{g/L}$, the stripping current increased with MBT concentration up to 100 $\mu\text{g/L}$ and then decreased for both metals. This is due to the fact that high concentration of MBT could block the mass transfer of metal ions at electrodeposition sites. The MBT concentration of 200 $\mu\text{g/L}$ was therefore selected for further experiments.

Scan rate

The stripping scan rate was changed from 50 to 300 mV/s. The stripping peak height was found to increase with the scan rate from 50 to 250 mV/s as shown in Figure 6. Under the criteria of peak shapes, 250 mV/s is chosen for the further study.

For equilibration time, step potential and pulse amplitude, the optimization value based on the greater current was selected.

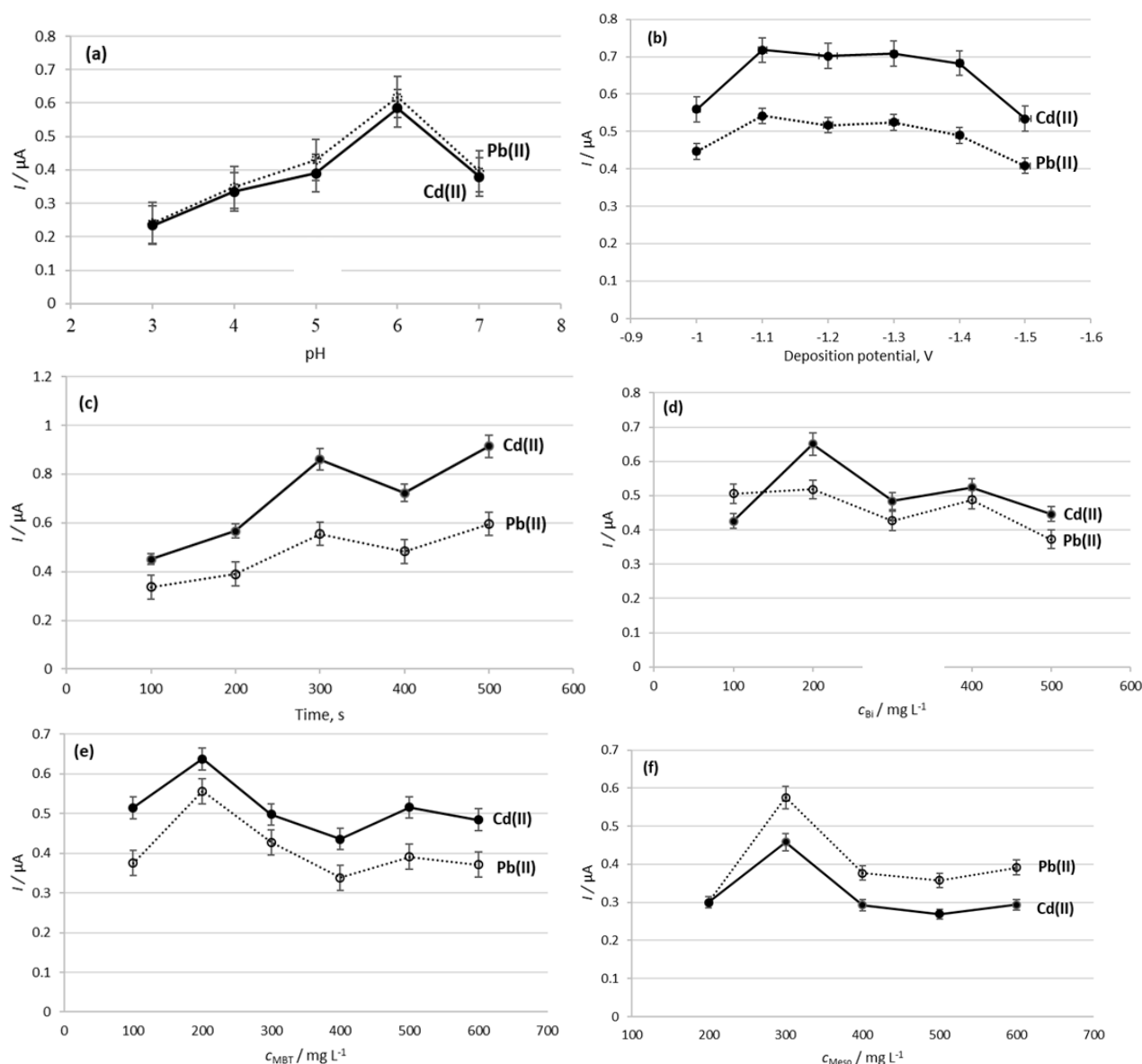


Figure 5. Effects of pH (a), deposition potential (b), deposition time (c), Bi concentration (d), Meso concentration (e) and MBT concentration (f) on stripping peak currents of 20 $\mu\text{g/L}$ Cd(II) and Pb(II).

All aforementioned optimized parameters are summarized in Table 2 and used in further experiments.

Table 2. Summary of optimized operating conditions

Parameter	Studied Range	Optimum Value
Deposition potential, V	-0.1 – -1.5	-1.1
Deposition time, s	100 – 500	300
pH	3 – 7	6
Bi concentration, $\mu\text{g/L}$	100 – 500	200
MBT concentration, $\mu\text{g/L}$	100 – 600	200
Meso concentration, $\mu\text{g/L}$	100 – 600	300
Equilibration time, s	10 – 50	30
Step potential, mV	1 – 20	5
Pulse amplitude, mV	25 – 80	75
Scan rate, mV / s	50 – 300	250

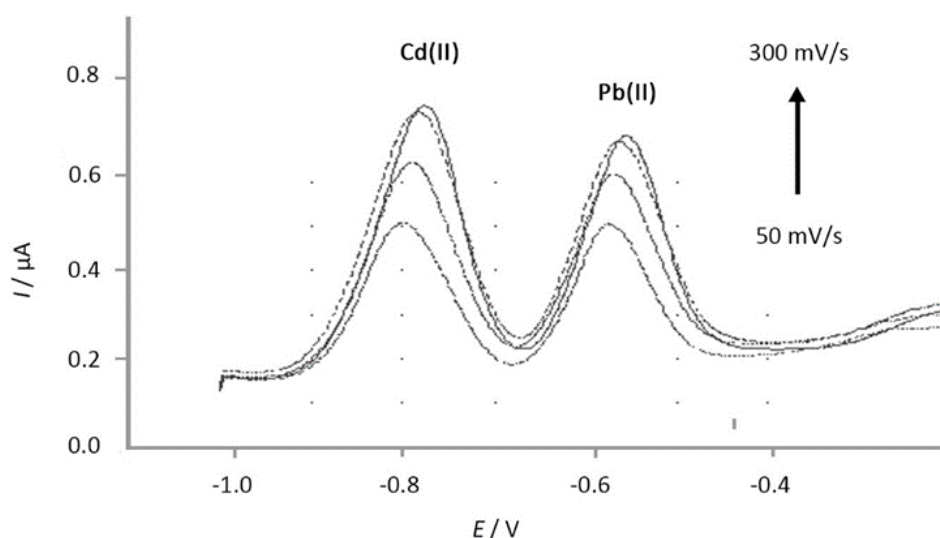


Figure 6. Effect of scan rate on stripping currents for concentrations of Pb(II) and Cd(II) 0.1 mg/L, Bi 200 μg/L, MBT 200 μg/L, Meso 300 μg/L.

Analytical performance

SWASV was used for simultaneous determination of Cd(II) and Pb(II) with the modified electrode Bi-Meso-MBT/GCE performed under optimized conditions to obtain current signals. The results for certain typical concentrations of Cd(II) and Pb(II) are shown in Figure 7 and the corresponding calibration curves are presented in Figure 8. The linearity in the range of 5-50 μg/L is observed for both metals with the correlation coefficient of 0.9978 for Cd(II) and 0.9960 for Pb(II), respectively. The linear regression equations of $i_p = 0.0142x + 0.0372$ (i_p : μA, x : μg/L) for Cd(II) and $i_p = 0.0113x - 0.0699$ for Pb(II) are defined. The limits of detection are found to be 0.56 μg/L for Cd(II) and 0.80 μg/L for Pb(II) by $3N/m$, where N is the standard deviation of replicate ($n=10$) responses of 5 μg/L of both metals taken as blank and m is the slope of the calibration curve. The limits of quantification, LOQ, defined as $10 N/m$, are determined as 1.87 μg/L for Cd(II) and 1.66 μg/L for Pb(II). The relative standard deviations were 2.97 % for Cd(II) and 2.04 % for Pb(II) with repetitive determinations ($n=10$) of 20.0 μg/L. All prove that the proposed method is satisfactorily reproducible and reliable for simultaneous determination of Cd(II) and Pb(II) at trace level and can be applied to real samples.

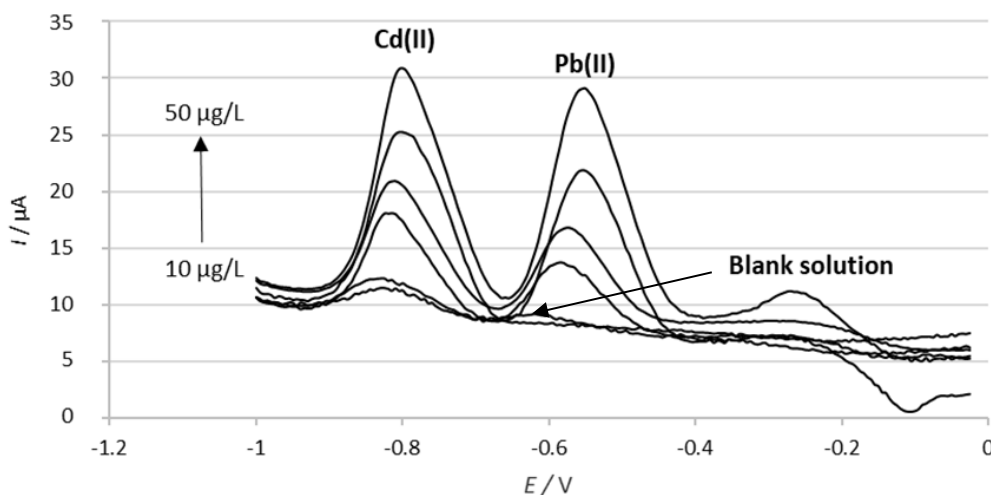


Figure 7. Typical SWASV voltammograms of water samples after spiking with 5 (as a blank) to 50 μg/L of both Cd(II) and Pb(II) standard solutions. Conditions: accumulation potential -1.1 V, accumulation time 300 s, acetate buffer solution pH 6, and scan rate 250 mV/s.

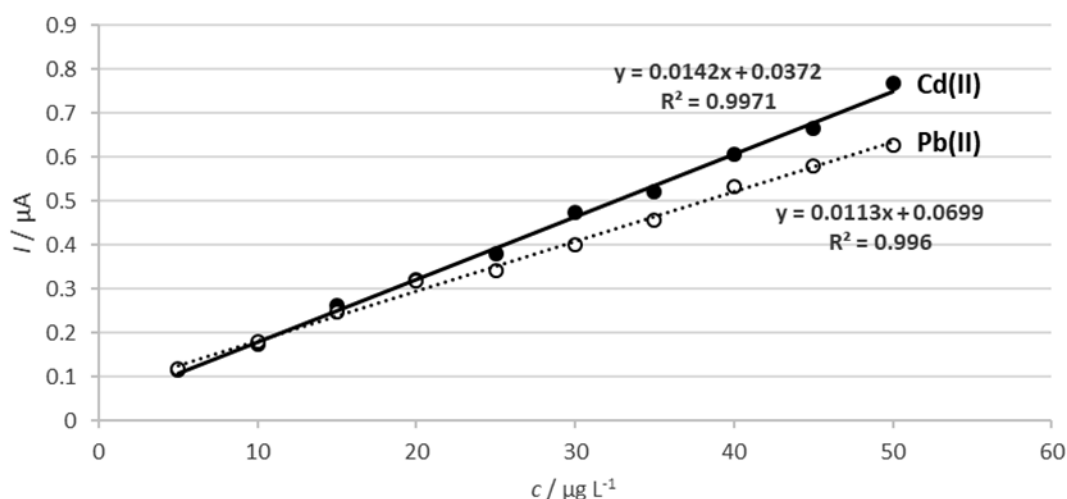


Figure 8. Calibration curves for Cd(II) and Pb(II) obtained by the proposed method.

Effect of other ions

Due to the capability of MBT to coordinate with a number of metal ions, the level of interference both from each other and other metal ions was investigated by the developed method under optimized conditions and the results are shown in Table 3. With the increase of Pb(II) concentration, no significant interference was observed for Cd(II) peak current. Other ions including Ca(II), Mg(II), Zn(II), Mn(II), Fe(II), Cu(II) and Al(III) at 1000 $\mu\text{g/L}$ were found to provide not high contributions for both metals. The most interfering ions here if present at high concentration are Cu(II) and Co(II) which normally can be masked by using a suitable and effective complexing agent such as ferrocyanide before analysis.

Table 3. Interference study of the stripping current measurements of 20 $\mu\text{g/L}$ Cd(II) and Pb(II) at Bi/Meso-MBT/GCE in the absence and presence of interfering metal ions

Interference	Contribution, % ^a ($I_p(\text{Cd(II)}) = 100\%$)	Contribution, % ^a ($I_p(\text{Pb(II)}) = 100\%$)
Cu(II)	-47.17	-21.78
Zn(II)	-16.68	-13.44
Mg(II)	37.49	14.98
Ca(II)	0.48	-3.68
Al(III)	2.34	-7.63
Mn(II)	13.36	0.65
Co(II)	-34.68	-40.14
Fe(III)	5.29	7.51
Ni(II)	-4.37	-5.87

^aContribution = $[(I_p \text{ with interferent} - I_p \text{ without interferent}) / I_p \text{ without interferent}] \times 100$

Certified reference material determination, method comparison and real sample analysis

The proposed method was applied to a certified reference material, natural water SRM 1640 from the National Institute of Standards and Technology (NIST), USA. As shown in Table 4, satisfactory recoveries, of 98.02 % for Cd(II) and 97.74 % for Pb(II) were obtained.

The proposed method was then used in the analysis of Cd(II) and Pb(II) in tap water samples collected from 11 sites in Hatyai city. Typical results of 5th and 6th regions are compared with ICP-OES results and summarized in Table 5, reflecting good agreement between here proposed and standard methods.

Table 4. Recovery of Cd(II) and Pb(II) for certified reference material determination

Concentration, µg/L		Concentration, µg/L		Error, %		Recovery, %	
Certified		Determined ^a					
Cd(II)	Pb(II)	Cd(II)	Pb(II)	Cd(II)	Pb(II)	Cd(II)	Pb(II)
22.79±0.96	27.89±0.14	22.34±0.010 (RSD = 2.97 %)	27.26±0.005 (RSD = 2.04 %)	1.97	2.25	98.02	97.74

^a Mean ± Standard deviation (n = 5)

Table 5. Determination of Cd(II) and Pb(II) in tap water samples (n = 4)

Sample	Concentration of spiked solution, µg/L	Concentration from the proposed method, µg/L ^b		Recovery, %		Concentration from ICP-OES, µg/L ^b		Difference, % ^d	
		Cd(II)	Pb(II)	Cd(II)	Pb(II)	Cd(II)	Pb(II)	Cd(II)	Pb(II)
Tap Water 5 ^a	0	ND ^c	ND	-	-	ND	ND	ND	ND
	5	5.11±0.003	5.12±0.005	-	-	5.10±0.1	5.30±0.12	1.00	3.45
	10	10.19±0.010	10.20±0.007	100.8	100.8	10.15±0.12	10.50±0.20	0.4	2.9
	20	20.40±0.012	20.35±0.010	101.4	101.1	20.35±0.021	20.50±0.25	0.25	0.7
	30	30.50±0.022	30.47±0.016	101.3	101.2	30.40±0.023	30.60±0.19	0.33	0.42
Tap Water 6 ^a	0	ND	ND	-	-	ND	ND	ND	ND
	5	5.16±0.004	5.15±0.006	-	-	5.10±0.02	5.03±0.400	1.17	2.36
	10	10.23±0.006	10.22±0.01	100.7	100.7	10.11±0.100	10.5±0.120	1.18	2.70
	20	20.36±0.012	20.33±0.01	101	100.9	20.01±0.002	20.04±0.05	0.15	0.14
	30	30.5±0.012	30.40±0.01	101.1	100.8	30.40±0.020	30.20±0.06	0.32	0.66

^aWater sample from 5th and 6th regions were selected for standard addition test; ^bMean ± Standard deviation (n = 4);

^cNot detected; ^dDifference of the concentration from the proposed method and that from ICP-OES

For real sample analysis with water from the 1st, 5th and 6th regions used as typical samples, the recoveries values were found to be 100.7-101.4 % for Cd(II) and 100.8-101.2 % for Pb(II) as shown in Table 6.

Table 6. Recovery test for the proposed method using tap water samples (n = 3)

Sample	Concentration of spiked solution, µg/L	Concentration found, µg/L		Recovery, %	
		Cd(II)	Pb(II)	Cd(II)	Pb(II)
Tap water 1 st region	0	ND	ND	-	-
	5	5.15±0.07	5.19±0.067	-	-
	10	10.23±0.002	10.25±0.008	100.8	100.6
	20	20.31±0.015	20.27±0.011	100.8	100.4
	30	30.35±0.011	30.36±0.015	100.4	100.5
Tap water 5 th region	0	ND	ND	-	-
	5	5.11±0.003	5.12±0.005	-	-
	10	10.19±0.01	10.20±0.007	100.8	100.8
	20	20.40±0.012	20.35±0.010	101.4	101.1
	30	30.50±0.022	30.47±0.016	101.3	101.2
Tap water 6 th region	0	ND	ND	-	-
	5	5.16±0.004	5.15±0.006	-	-
	10	10.23±0.006	10.22±0.01	100.7	100.7
	20	20.36±0.012	20.33±0.01	101.0	100.9
	30	30.50±0.012	30.40±0.01	101.1	100.8

Mean ± S.D. (n = 3); ND: Not detected

As shown in Table 7, the results obtained with here proposed method are comparable with the results obtained by other anodic stripping voltammetric based methods. It is clear, however, that

here proposed method has the advantage of wider linear range, lower detection limits and greater simplicity. The only disadvantage could be a little longer deposition time, which can be adjusted according to the required accuracy. Other very recent methods without using bismuth are also included (Entry 1-6) as references to show that here proposed method is reasonably satisfactory.

Table 7. Comparison of the proposed method for determination of Cd(II) and Pb(II) in water sample with other recent anodic stripping voltammetric methods

Entry	Electrodes	Method	Deposition time, s	Linear range of concentration, $\mu\text{g/L}$		LOD, $\mu\text{g/L}$		Ref
				Cd(II)	Pb(II)	Cd(II)	Pb(II)	
1	HMgFe-EDG/G	SWASV	180	11.2 – 207	11.2 – 207	1.22	0.304	[34]
2	ST PANI NTs	SWASV	600	0.207 – 24.84	1.12 – 19.04	0.02	0.03	[35]
3	CA/RGO/GCE	SWASV	1500	0.0207 – 2.07	0.112 – 13.44	0.004	0.002	[36]
4	Nafion/CLS/PGR/GCE	SWASV	140	10.35 – 1035	5.60 – 560	2.06	0.336	[37]
5	GO/ κ -Car/L-Cys/GCE	SWASV	120	1.03 – 10.35	0.56 – 5.60	0.12	0.12	[38]
6	NCQDs-GO	DPASV	300	10.35 – 20.7	0.112 – 11200	1.16	7.4	[39]
7	In situ Bi/Graphite/Epoxy	SWASV	120	41.4 – 352	56 – 280	14.5	5.60	[40]
8	Bi-Meso-MBT/GCE	SWASV	300	5 - 50	5 – 50	0.56	0.80	This work

HMgFe-EDH/G:	Hierarchical MgFe-layered double hydroxide microsphere graphene composite
ST PANI NTs:	Size-tunable polyaniline nanotube-modified electrode
CA/RGO/GCE:	calixarene functionalized reduced graphene oxide
CLS/PGR:	calcium lignosulphonate functionalized porous graphene nanocomposite
GO/ κ -Car/L-Cys/GCE:	graphene oxide κ -carrageenan L-cysteine nanocomposite
NCQDs-GO:	N-doped carbon quantum dots graphene oxide hybrid
In situ Bi/Graphite/Epoxy:	in situ bismuth film on graphite dispersed in epoxy resin
Bi-Meso-MBT/GCE:	Bismuth mesoporous silica 2-mercaptopbenzothiazole modified GCE

Conclusions

GCE was modified with Bi, Meso and MBT and applied to simultaneous determination of Cd(II) and Pb(II) in trace levels, using square wave anodic stripping voltammetry (SWASV). The method provides satisfactory advantages of speed, simplicity, sensitivity and selectivity. Good recoveries of Cd(II) (100.7 %) and Pb(II) (100.8 %) were obtained for the real sample, along with LOD of 0.56 $\mu\text{g/L}$ for Cd(II) and 0.80 $\mu\text{g/L}$ for Pb(II), respectively. The method can be used satisfactorily for the analysis of tap water in local areas and the results were found in good agreement with those obtained by ICP-OES.

References

- [1] V. Karri, M. Schuhmacher, V. Kumar, *Environmental Toxicology and Pharmacology* **48** (2015) 203-213.
- [2] C. Yvonne H, M. P. Wilkie, *Aquatic Toxicology* **161** (2015) 176-188.
- [3] United States Environmental Protection Agency, <http://water.epa.gov/drink/contaminants/index/cfm> (13th September 2017)
- [4] Q. Hu, G. Yang, Y. Zhao, J. Yin, *Analytical and Bioanalytical Chemistry* **375** (2003) 831-835.
- [5] S. Xu, S. Xu, Y. Zhu, W. Xu, P. Zhou, C. Zhou, B. Dong, H. Song, *Nanoscale* **6** (2014) 12573-12579.
- [6] M. Fouskaki, N. A. Chaniotakis, *Analytical Chemistry* **77** (2005) 1780-1784.
- [7] R. Liu, P. Liang, *Journal of Hazardous Materials* **152** (2008) 166–171.
- [8] G. Abbasse, B. Ouddane and J. C. Fischer, *Journal of Analytical Atomic Spectrometry* **17** (2002) 1354-1358.
- [9] N. Pourreza, S. Rastegarzadeh, A. Larki, *Journal of Industrial and Engineering Chemistry* **20** (2014) 2680-2686.

- [10] D. V. Biller, K. W. Bruland, *Marine Chemistry* **130-131** (2012) 12-20.
- [11] P. Chooto, Modified electrodes for determining trace metal ions. In: Application of the Voltammetry. M. Stoytcheva, R. Zlatev, Ed(s)., Intech, Rijeka, Croatia: InTech; 2017 p. 129
- [12] P. Chooto, P. Wararatananurak, C. Innuphat, *ScienceAsia* **36** (2010) 150-156.
- [13] C. Innuphat, P. Chooto, *ScienceAsia* **43** (2017) 33-41.
- [14] S. Cerovac, V. Guzsány, Z. Kónya, A. M. Ashrafi, I. Švancara, S. Rončević, Á. Kukovecz, B. Dalmacija, K. Vytřas, *Talanta* **134** (2015) 640-649.
- [15] D. Li, J. Jia, J. Wang, *Talanta* **83** (2010) 332-336.
- [16] L. Xiao, B. Wang, L. Ji, F. Wang, Q. Yuan, G. Hu, A. Dong, W. Gan, *Electrochimica Acta* **222** (2016) 1371-1377.
- [17] Y. Zuo, J. Xu, F. Jiang, X. Duan, L. Lu, H. Xing, T. Yang, Y. Zhang, G. Ye, Y. Yu, *Journal of Electroanalytical Chemistry* **801** (2017) 146-152.
- [18] M. Arab Chamjangali, H. Kouhestani, F. Masdarolomoor, H. Daneshinejad, *Sensors and Actuators B Chemical* **216** (2015) 384-393.
- [19] Y. Wu, N. B. Li, H. Q. Luo, *Sensors and Actuators B* **133** (2008) 677-681.
- [20] K. Keawkim, S. Chuanuwatanakul, O. Chailapakul, S. Motomizu, *Food Control* **31** (2013) 14-21.
- [21] N. Serrano, A. G. Calabuig, M. del Valle, *Talanta* **138** (2015) 130-137.
- [22] H. Dai, N. Wang, D. Wang, H. Ma, M. Lin, *Chemical Engineering Journal* **299** (2016) 150-155.
- [23] S. Kheirandish, M. Ghaedi, K. Dashtian, R. Jannesar, M. Montazerzohori, F. Pourebrahim, M. A. Zare, *Journal of Colloid and Interface Science* **500** (2017) 241-252.
- [24] L. Zhu, L. Xu, B. Huang, N. Jia, L. Tan, S. Yao, *Electrochimica Acta* **115** (2014) 471-477.
- [25] J. P. Llovera, C. P. Ràfols, N. Serrano, J. M. Díaz-Cruz, C. Ariño, M. Esteban, *Talanta* **175** (2017) 501-506.
- [26] Z. Guo, D. Li, X. Luo, Y. Li, Q. N. Zhao, M. Li, Y. Zhao, T. Sun, Chi Ma, *Journal of Colloid and Interface Science* **490** (2017) 11-22.
- [27] I.P. Khullar, U. Agarwala, *Canadian Journal of Chemistry* **53** (1975) 1165-1171.
- [28] Ş. Tokaloğlu, A. Papak, Ş. Kartal, *Arabian Journal of Chemistry* **10** (2017) 19-23.
- [29] V. S. Somerset, M. J. Klink, M. M. C. Sekota, P. G. L. Baker, E. I. Iwuoha, *Analytical Letters* **39** (2006) 1683-1698.
- [30] M. d. F. B. Sousa, E. J. Dallan, S. B. Yamaki, R. Bertazzoli, *Electroanalysis* **9** (1997) 614-618.
- [31] H. Huang, W. Zhu, X. Gao, X. Liu, H. Ma, *Analytica Chimica Acta* **947** (2016) 32-41.
- [32] [Chemicaland21.com](http://chemicalland21.com), <http://chemicalland21.com/specialtychem/perchem/2-MERCAPTOBENZOTHIAZOLE.htm> (29th May 2018)
- [33] L. Cao, J. Jia, Z. Wong, *Electrochimica Acta* **53** (2008) 2177-2182.
- [34] Y. Ma, Y. Wang, D. Xie, Y. Gu, X. Zhu, H. Zhang, G. Wang, Y. Zhang, H. Zhao, *Chemical Engineering Journal* **347** (2018) 953-962.
- [35] G. Zhu, Y. Ge, Y. Dai, X. Shang, J. Yang, J. Liu, *Electrochimica Acta* **268** (2018) 202-210.
- [36] C. Göde, M. L.i Yol, A. Yilmaz, N. Atar, S. Wang, *Journal of Colloid and Interface Science* **508** (2017) 525-531.
- [37] L. Yu, Q. Zhang, B. Yang, Q. Xu, Q. Xu, X. Hu, *Sensors and Actuators B* **259** (2018) 540-551.
- [38] T. Priya, N. Dhanalakshmi, S. Thennarasu, N. Thinakaran, *Carbohydrate Polymers* **182** (2018) 199-206.
- [39] L. Li, D. Liu, A. Shi, T. You, *Sensors and Actuators B* **255** (2018) 1762-1770.
- [40] K. Pokpas, S. Zbeda, N. Jahed, N. Mohamed, P. G. Baker, E. I. Iwuoha, *International Journal of Electrochemical Science* **9** (2014) 736-759.